AMERICAN SOCIETY FOR MICROBIOLOGY | Molecular and Cellular Biology

Intercellular Communication between Keratinocytes and Fibroblasts Induces Local Osteoclast Differentiation: a Mechanism Underlying Cholesteatoma-Induced Bone Destruction

Yoriko Iwamoto,[a,b,c] Keizo Nishikawa,[b,c,d] Ryusuke Imai,[a,e] Masayuki Furuya,[b,c,f] Maki Uenaka,[b,c] Yumi Ohta,[a] Tetsuo Morihana,[a] Saori Itoi-Ochi,[e] Josef M. Penninger,[g] Ichiro Katayama,[e] Hidenori Inohara,[a] Masaru Ishii[b,c,d]

Department of Otorhinolaryngology-Head and Neck Surgery, Graduate School of Medicine, Osaka University, Osaka, Japan[a]; Department of Immunology and Cell Biology, Graduate School of Medicine and Frontier Biosciences, Osaka University, Osaka, Japan[b]; WPI-Immunology Frontier Research Center, Osaka University, Osaka, Japan[c]; JST, CREST, Tokyo, Japan[d]; Department of Dermatology, Graduate School of Medicine, Osaka University, Osaka, Japan[e]; Department of Orthopedic Surgery, Graduate School of Medicine, Osaka University, Osaka, Japan[f]; Institute of Molecular Biotechnology, Austrian Academy of Sciences, Vienna, Austria[g]

Bone homeostasis is maintained by a balance in activity between bone-resorbing osteoclasts and bone-forming osteoblasts. Shifting the balance toward bone resorption causes osteolytic bone diseases such as rheumatoid arthritis and periodontitis. Osteoclast differentiation is regulated by receptor activator of nuclear factor κB ligand (RANKL), which, under some pathological conditions, is produced by T and B lymphocytes and synoviocytes. However, the mechanism underlying bone destruction in other diseases is little understood. Bone destruction caused by cholesteatoma, an epidermal cyst in the middle ear resulting from hyperproliferation of keratinizing squamous epithelium, can lead to lethal complications. In this study, we succeeded in generating a model for cholesteatoma, epidermal cyst-like tissue, which has the potential for inducing osteoclastogenesis in mice. Furthermore, an *in vitro* coculture system composed of keratinocytes, fibroblasts, and osteoclast precursors was used to demonstrate that keratinocytes stimulate osteoclast differentiation through the induction of RANKL in fibroblasts. Thus, this study demonstrates that intercellular communication between keratinocytes and fibroblasts is involved in the differentiation and function of osteoclasts, which may provide the molecular basis of a new therapeutic strategy for cholesteatoma-induced bone destruction.

Bone is a highly dynamic organ in which homeostasis is maintained by a balance in activity between bone-resorbing osteoclasts and bone-forming osteoblasts. An imbalance between osteoclastic and osteoblastic activity causes various skeletal disorders. Osteoclasts are multinucleate cells that differentiate from mononuclear macrophage/monocyte-lineage hematopoietic precursor cells, which are attracted to the bloodstream by factors, including sphingsine-1 phosphate (1, 2). Osteoclast differentiation and function are regulated by macrophage colony-stimulating factor (M-CSF) and receptor activator of nuclear factor κB ligand (RANKL) (3–5). Under physiological conditions, osteoblasts or osteocytes are the source of RANKL (6–8). RANKL-mediated osteoclastogenesis also plays an important role in bone destruction in inflammatory bone diseases such as rheumatoid arthritis (RA) or periodontal diseases. In such pathological states, synoviocytes or immune cells, such as B or T lymphocytes, infiltrating into the area are proposed to be the major sources of RANKL (9–11). In RA, infiltration of T helper 17 (Th17) cells is observed in the synovium. Th17 cells indirectly induce RANKL expression in synoviocytes by producing interleukin-17 (IL-17) (12), and Th17 cells themselves express RANKL on their plasma membrane (13). Thus, in many bone destructive diseases, the mechanisms of bone destruction are becoming clarified in detail. However, there are still certain bone destructive diseases whose underlying mechanisms remain to be elucidated. Cholesteatoma, a benign entity arising in temporal bone, is one such disease where our understanding is limited.

Cholesteatoma is an epidermal cyst occurring in the middle ear (14, 15), which consists of three layers: perimatrix, matrix, and cystic content. Matrix is composed of keratinizing stratified squamous epithelium. Perimatrix contains collagen fibers and fibroblasts. Cystic content is made up of keratinaceous debris. Advanced cholesteatoma can cause the destruction of bone, which results in severe complications, such as facial nerve palsy, meningitis, and brain abscess. Although recent developments in antibiotics along with early detection have decreased the incidence of severe complications, these complications still occur if cholesteatoma is not treated properly. Currently, the only effective treatment is complete surgical eradication of cholesteatoma; however, postoperative recurrence is possible. In the perimatrix layer, inflammatory cell infiltration is usually observed, and inflammation is known to be an exacerbating factor for cholesteatoma. In contrast, inflammation alone does not cause bone destruction because chronic suppurative otitis media, which is a chronic inflammatory state in middle ear mucosa, rarely causes bone destruction (16, 17). Therefore, it is suggested that proliferation of the kera-

Received 25 November 2015 **Returned for modification** 16 December 2015
Accepted 7 March 2016

Accepted manuscript posted online 21 March 2016

Citation Iwamoto Y, Nishikawa K, Imai R, Furuya M, Uenaka M, Ohta Y, Morihana T, Itoi-Ochi S, Penninger JM, Katayama I, Inohara H, Ishii M. 2016. Intercellular communication between keratinocytes and fibroblasts induces local osteoclast differentiation: a mechanism underlying cholesteatoma-induced bone destruction. Mol Cell Biol 36:1610–1620. doi:10.1128/MCB.01028-15.

Address correspondence to Masaru Ishii, mishii@icb.med.osaka-u.ac.jp.

Supplemental material for this article may be found at http://dx.doi.org/10.1128/MCB.01028-15.

tinized epithelial layer plays an important role in bone destruction.

Recently it has been reported that cell differentiation, proliferation, and tissue homeostasis within cholesteatoma are maintained by interactions between matrix-keratinocytes and perimatrix-fibroblasts (18). Keratinocyte-derived interleukin-1 (IL-1) induces fibroblasts to secrete some cytokines, such as transforming growth factor α (TGF-α) (19) or keratinocyte growth factor (KGF) (20). These cytokines in turn support the proliferation and differentiation of keratinocytes (21).

In this study, we investigated whether the interactions between keratinocytes and fibroblasts affect bone destruction. Accordingly, we reconstructed the interactions *in vivo* and *in vitro*, using mouse ear pinna-derived keratinocytes and fibroblasts. Using this model, we revealed that the interaction between keratinocytes and fibroblasts induces osteoclastogenesis, which can lead to bone resorption.

MATERIALS AND METHODS

Mice and animal experiments. C57BL/6 mice (referred to as wild-type [WT] mice) were purchased from CLEA Japan. CAG-enhanced green fluorescent protein (EGFP) mice were purchased from Charles River. Tartrate-resistant acid phosphatase (TRAP)-tdTomato transgenic mice were generated previously and genotyped as previously described (22). Myeloid differentiation primary response (Myd88) knockout mice were generated previously (23). *Tnfsf11* knockout mice were generated previously (24). CAG-tdTomato mice were obtained by crossing B6.Cg-Gt (ROSA)26Sortm9(CAG-tdTomato)Hze/J mice (The Jackson Laboratory) and CAG-Cre transgenic mice (25). All strains were on the C57BL/6 background. Both male and female mice were used except when indicated otherwise. Animal experiments were conducted in a blinded fashion with respect to the investigator. Animals were randomly included in the experiments according to genotyping results. The numbers of animals used per experiment are stated in the figure legends. All mice were born and maintained under specific-pathogen-free conditions, and all animal studies were approved by the Institutional Animal Care and Use Committee of Osaka University.

Cell culture. For the isolation of keratinocytes and fibroblasts, ear pinnae were treated with dispase (4 mg/ml) for 1 h and separated into dermis and epidermis. The epidermis was treated with TrypLE express enzyme (Thermo Fisher Scientific) at 37°C for 5 min, and the resulting single-cell suspension was used as keratinocytes. Dermis was treated with dispase (4 mg/ml) and collagenase (3 mg/ml) at 37°C for 2 h, and obtained cells were plated in a 10-cm dish and cultured in Dulbecco's modified Eagle's medium (DMEM) (Nacalai Tesque) supplemented with 10% fetal bovine serum (FBS). The cells were passaged 3 to 7 times and used as ear pinna-derived fibroblasts. For three-dimensional (3D) culture of keratinocytes, keratinocytes were isolated from ear pinnae of mice as described above. Cells were seeded for culture in CnT-Prime epithelial culture medium (CnT-PR; CELLnTEC) at a density of 3.3×10^5 cells/cm^2 in Millicell PCF 0.4-μm inserts (Millipore). Four inserts were placed in a 6-cm petri dish. When cells reached confluence, the medium was switched to defined epidermal keratinocyte 3D prime medium (CnT-02 3D) or CnT-Prime 3D barrier culture medium (CnT PR3D; CELLnTEC) to induce differentiation of keratinocytes. After 12 h, medium in the inserts was aspirated and the cells were then cultured at the air-liquid interface for more than 10 days. Medium was changed every 2 days, and after more than 10 days these media were used as keratinocyte supernatants. For *in vitro* culture, keratinocytes and fibroblasts derived from CAG-EGFP mice were used except when indicated otherwise. Ear pinna-derived fibroblasts were cultured in DMEM with or without lipopolysaccharides (250 ng/ml) from *Escherichia coli* (Sigma-Aldrich) for 2 days. Ear pinna-derived fibroblasts were cultured for 2 days in CnT PR3D medium with or without recombinant mouse galectin-3 (10 μg/ml; R&D Systems), Cxcl-1 (200 ng/ml; Bio Legend), vascular endothelial growth factor 164 (VEGF-164; 100 ng/ml; BioLegend), Cxcl-16 (100 ng/ml; PeproTech), and prostaglandin E_2 (PGE_2; 10 μM; Cayman Chemical). Neonatal mouse calvarial osteoblasts were isolated as described previously (26).

***In vitro* coculture assay.** Ear pinna-derived fibroblasts on 24-well plates were cocultured with Millicell PCF 0.4-μm inserts with keratinocytes cultured for more than 10 days. Inserts with fibroblasts seeded in DMEM supplemented with 10% FBS at a density of 2.5×10^4 cells/cm^2 and cultured for 2 days or inserts lacking cells were used as controls. Two days after coculture, each insert was removed and fibroblasts were further cocultured with bone marrow-derived monocyte-macrophage precursor cells (BMMs) in the presence of 10 ng/ml macrophage-colony-stimulating factor (M-CSF) (R&D Systems) for 3 days. Bone marrow-derived cells cultured with 10 ng/ml M-CSF for 3 days were used as BMMs (27–29). BMMs derived from TRAP-tdTomato mice were used in this study. Three days after coculture, osteoclastogenesis was evaluated using the TRAP solution assay, as previously described (30).

Establishment of epidermal cyst-like mass. The methods for the isolation of ear pinna-derived keratinocytes and fibroblasts were described above. Keratinocytes (4×10^6 cells) and fibroblasts (8×10^5 cells) were mixed in 100 μl phosphate-buffered saline (PBS) and injected under the periosteum of calvarial bone percutaneously. The injection of keratinocytes (4×10^6 cells) in 100 μl PBS was used as a control.

Histology, immunohistochemistry, and confocal imaging. For frozen sections, mice were perfused with 4% paraformaldehyde (PFA) with 20% sucrose for fixation, and dissected bone tissues were further fixed with 4% PFA and 20% sucrose for 4 h at 4°C followed by a 7-day decalcification in 10% EDTA, and then they were embedded in OCT compound (Sakura Finetek). Sections, 10 μm thick, were prepared using Kawamoto's film method. Sections were mounted with Vectashield mounting medium with 4′,6-diamidino-2-phenylindole (DAPI) (Vector Laboratories, Inc.), and images were acquired with an A1 confocal microscope (Nikon). For paraffin-embedded sections, freshly dissected calvarial bones were fixed in 4% PFA overnight, followed by a 7-day decalcification in 10% EDTA. Sections (3 μm thick) were stained with hematoxylin and eosin (H&E) using a standard protocol. The maximum diameter of the lesion mass was calculated using ImageJ software. The number of concentric nodules was calculated manually. For immunohistochemical analysis, sections were blocked with normal rabbit serum for 30 min. After antigen retrieval for 10 min in Tris-EDTA (pH 9.0) in a 110°C oil bath, endogenous peroxidase activity was quenched with 0.3% H_2O_2 for 30 min. Sections were then stained overnight at 4°C with anti-RANKL (1:400; Santa Cruz), anti-cytokeratin 14 (anti-CK14) (1:500; Thermo Scientific), and anti-CK10 (1:500; BioLegend). A Vectastain elite ABC kit (Vector Laboratories, Inc.) and the protocol provided by the manufacturer were used. Sections were counterstained with hematoxylin for 30 s before mounting with Paramount-N (Falma, Japan). Goat IgG (1:800; Santa Cruz), rabbit IgG (1:200; Santa Cruz), and mouse IgG1 (1:250; Dako) were used as the isotype controls.

Image data analysis. For calculating the ratio of osteoclast surface to bone surface, EGFP-positive areas and tdTomato-positive areas were automatically detected by NIS element software (Nikon). Bone surface length under the EGFP-positive mass lesion and tdTomato-positive osteoclast surface length were calculated manually using ImageJ software.

Immunoblot analysis. Whole-cell extracts of fibroblasts were prepared by lysis in radioimmunoprecipitation assay buffer and subjected to immunoblot analysis using anti-RANKL (1:1,000; Santa Cruz) and anti-β-actin (1:1,000; GenScript), respectively.

RNA isolation and RT-qPCR. Total RNA and cDNA were prepared using Maxwell 16 LEV simplyRNA purification kits (Promega) and Superscript III reverse transcriptase (Thermo Fisher Scientific) according to the manufacturer's protocol. Quantitative real-time PCR (RT-qPCR) was performed with thermal cycler Dice real-time system TP800 (TaKaRa). The expression of every sample was calculated relative to that of the β-actin housekeeping gene. Primer sequences are summarized in Table 1.

TABLE 1 Primer sequences for quantitative PCR

Gene	Sequence (5′–3′)	
	Forward	Reverse
Actb	CTTCTACAATGAGCTGCGTG	TCATGAGGTAGTCTGTCAGG
Tnfsf11	CAGCATCGCTCTGTTCCTGTA	CTGCGTTTTCATGGAGTCTCA
Tnfsf11b	ACCCAGAAACTGGTCATCAGC	CTGCAATACACACACTCATCACT
Tlr4	ATGGCATGGCTTACACCACC	GAGGCCATTTTGTCTCCACA
Lgals3	GCCTACCCCAGTGCTCCT	CTCATTGAAGCGGGGGTTA
Slpi	GGCCTTTTACCTTTCACGGTG	TACGGCATTGTGGCTTCTCAA
Plau	GCGCCTTGGTGGTGAAAAAC	TTGTAGGACACGCATACACCT
Vegfa	CAGGCTGCTGTAACGATGAA	TTTGACCCTTTCCCTTTCCT
Grn	TTCACACACGATGCGTTTCA	AGGGCACACGACAGAAAAAG
Cxcl16	ACCCTTGTCTCTTGCGTTCTTCCT	ATGTGATCCAAAGTACCCTGCGGT
Il9	ATGTTGGTGACATACATCCTTGC	TGACGGTGGATCATCCTTCAG
Cxcl1	CTGGGATTCACCTCAAGAACATC	CAGGGTCAAGGCAAGCCTC
Csf3	ATGGCTCAACTTTCTGCCCAG	CTGACAGTGACCAGGGGAAC

Cytokine array. Keratinocyte supernatant and fresh CnT-02 3D (CELLnTEC), as a control sample, were assessed using a cytokine antibody array I (biotin label based) for mouse, L-series (RayBiotech), according to the manufacturer's protocol. This multiplex assay measures 308 different cytokines on a glass chip format. Data were analyzed using microarray data analysis software (Filgen). The net intensity was calculated by subtracting the mean intensity of the local background area from the mean intensity of the spot areas.

Statistics. Statistical analysis was done using Welch's *t* test or ratio paired *t* test for comparisons between two groups, Kruskal-Wallis test with Dunn's multiple-comparison posttest, one-way analysis of variance (ANOVA) with Tukey's multiple-comparison posttest, or two-way ANOVA with Sidak's multiple-comparison posttest for comparisons among three or more groups as described in each figure legend.

RESULTS

Establishment of epidermal cyst-like mass lesions. Initially, we attempted to mimic the histology of epidermal cysts in mice, using keratinocytes and fibroblasts derived from mouse ear pinnae. Keratinocytes isolated from epidermis and fibroblasts isolated from dermis were mixed at a 5:1 ratio and injected under the calvarial periosteum (Fig. 1A). Three days after injection, a mass lesion was observed under the skin of the head. At 1 week after injection, the mass lesion with bone was dissected and histological analysis was performed (Fig. 1B and C). The 5:1 ratio was the most effective at inducing the mass lesion. Histological sections revealed that the obtained mass contained several round nodules with concentric layers (Fig. 1B and C). In their centers the nodules contained debris-like structures, and fibrous tissue was observed surrounding the nodules.

To examine the cell components in the mass lesion in detail, we separated keratinocytes and fibroblasts by using two mouse strains with different kinds of fluorescence labeling. We isolated keratinocytes from CAG-EGFP mice and fibroblasts from CAG-tdTomato mice (Fig. 2A). The concentric nodules expressed EGFP, indicating they were formed by keratinocytes. Fibroblasts expressing tdTomato surrounded these nodules and formed a single mass. The single EGFP-expressing cells and tdTomato-expressing cells were not mixed with each other. Similar histological appearances were observed at 2 and 4 days after injection

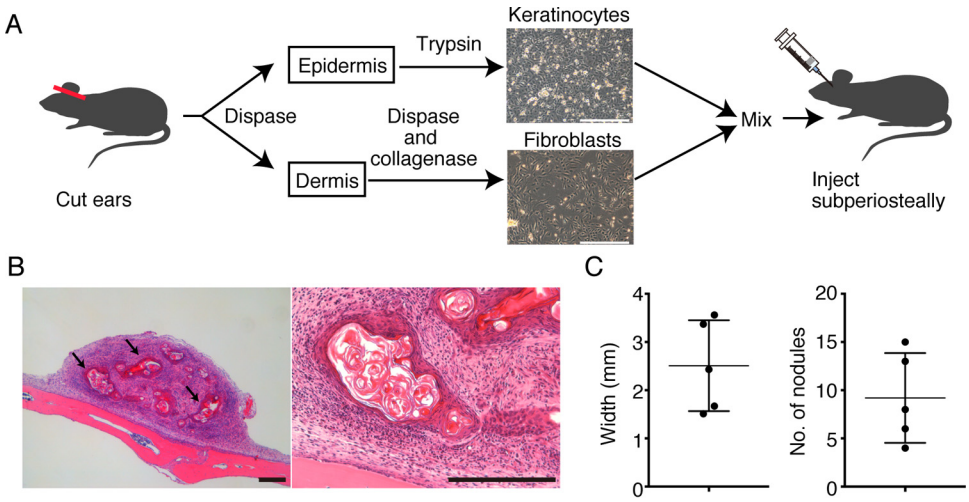

FIG 1 Establishment of a keratinocyte and fibroblast mixed cyst on calvarial bone. (A) Schematic description of the method for generating a mass lesion composed of ear pinna-derived keratinocytes and fibroblasts. Scale bars, 250 μm. (B) Histological analysis of the mass lesion with calvarial bone. Hematoxylin and eosin-stained histologic sections. Arrows indicate concentric nodules. Scale bars, 250 μm. Representative images of five experiments are shown. (C) The width and the number of nodules in a single section, calculated by ImageJ software. Data are presented as means ± standard deviations (SD).

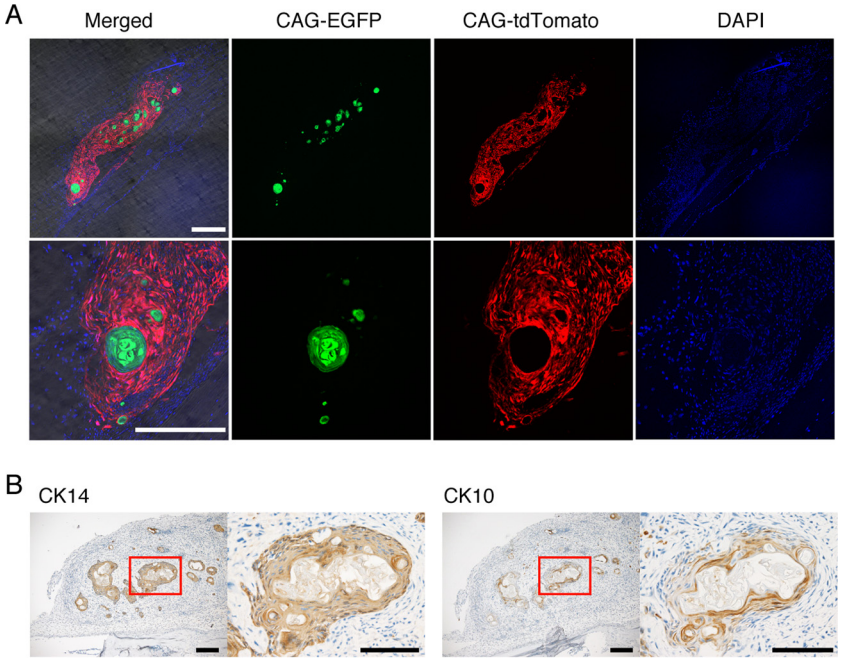

FIG 2 Experimental mass lesions are histologically similar to epidermal cysts. (A) Confocal images of calvarial sections from WT mice injected with keratinocytes derived from CAG-EGFP mice and fibroblasts derived from CAG-tdTomato mice at 7 days after injection. Scale bars, 250 μm. Representative images of three mice are shown. (B) Immunohistochemical analysis of keratinocyte differentiation markers CK10 and CK14. Hematoxylin staining was used as a counterstain (blue). Boxed regions in the images on the left are magnified in images on the right. Scale bars, 200 μm. Representative images of three mice are shown.

(Fig. 2A; also see Fig. S1A in the supplemental material), while the size of the cysts increased throughout development (see Fig. S1B). In order to further characterize the cells in the nodules, we examined the expression of keratinocyte differentiation markers. In normal skin, keratinocytes differentiate and migrate toward the surface of the epidermis, forming a multilayered epidermis and stratum corneum. Keratinocytes in the basal layer express cytokeratin 14 (CK14), and differentiated keratinocytes expressed CK10 (see Fig. S2). In the mass lesion, keratinocytes forming concentric nodules widely express CK14, whereas cells in the inner layer of the nodules expressed CK10. Therefore, the histology of the nodules resembles that of keratinized squamous epithelial cells (Fig. 2B; also see Fig. S2). Thus, we succeeded in inducing epidermal cyst-like tissue by transplantation of a mixture of keratinocytes and fibroblasts.

Epidermal cyst-like mass lesions induce osteoclasts on the calvarial bone surface. The next question we examined is whether or not this mass lesion has the potential to destroy bone. Previously, we generated TRAP-tdTomato mice whose osteoclasts expressed fluorescent tdTomato protein driven by the TRAP promoter (22). We examined the induction of osteoclasts on the bone surface by using TRAP-tdTomato mice as the recipients. EGFP-expressing keratinocytes and fibroblasts were individually injected into TRAP-tdTomato mice. The injection of keratinocytes resulted in keratinized nodules without fibroblastic layers (Fig. 3A). After transplantation, a mass lesion was observed in 4 out of 4 injections of keratinocytes and fibroblasts compared to 3 out of 5 injections of keratinocytes alone. The injection of fibroblasts alone did not result in mass lesions (data not shown). Histomorphometric analysis revealed that the ratio of osteoclast surface to bone surface under the EGFP-positive lesions was significantly higher in keratinocyte- and fibroblast-injected mice than in mice injected with keratinocytes alone (Fig. 3B). However, bone destruction was not detected by microcomputed tomography (data not shown). These results suggest that nodules can be formed by keratinocytes alone, whereas osteoclasts are induced only by keratinocyte-fibroblast mixed cysts.

In dermal tissues such as skin and ear pinna, RANKL was expressed in fibroblast-like cells rather than keratinocytes (see Fig. S3A in the supplemental material). This result prompted us to examine the source of RANKL in the epidermal cyst-like tissue. Immunohistochemistry revealed that fibroblasts expressed RANKL, while keratinocytes were only weakly stained (Fig. 3C; also see Fig. S3B). The expression was detected in the early stage of mass formation (see Fig. S3B). Fibroblasts around the epithelial layer had a tendency to show high-level expression of RANKL (Fig. 3C). These results suggest that interactions between keratinocytes and fibroblasts play a pivotal role in the induction of RANKL expression.

Soluble factors secreted by keratinocytes induce osteoclastogenesis. To further investigate the relationship among keratinocytes, fibroblasts, and osteoclast precursors, we established an *in vitro* coculture system composed of these cells (Fig. 4A). In order to examine the function of keratinocyte-fibroblast interactions in the induction of osteoclast differentiation, we performed coculture experiments using the ear pinna-derived fibroblasts and multiple layers of keratinocytes. The mRNA expression of *Tnfsf11* (encoding RANKL) was significantly elevated in fibroblasts cocultured with keratinocytes compared to that in cultures of fibroblasts or with empty inserts (Fig. 4B). RANKL expression was also detected in fibroblasts cultured with keratinocyte supernatant at both the mRNA and protein levels (Fig. 4C and D). The elevation of *Tnfsf11* peaked 36 h after stimulation. On the other hand, the

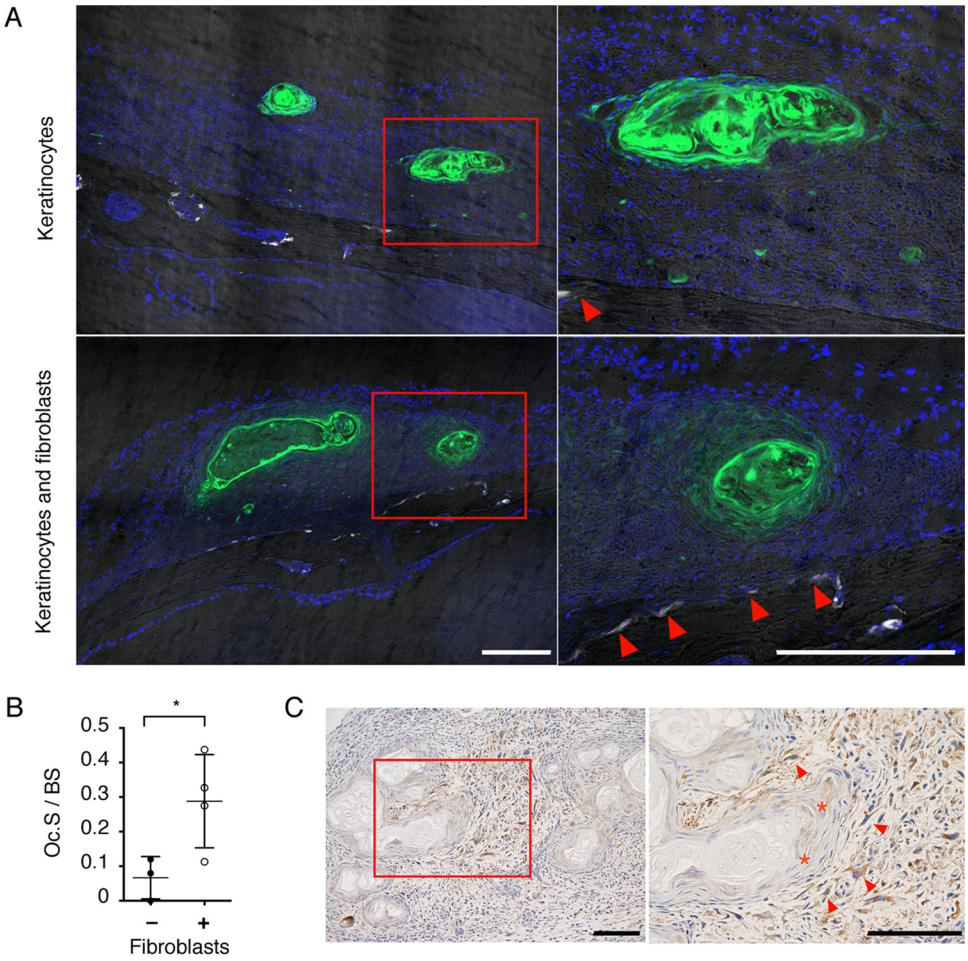

FIG 3 Epidermal cyst-like tissue induces differentiation of osteoclasts. (A) Histological analysis of calvarial sections of TRAP-tdTomato mice injected with EGFP-expressing keratinocytes alone (upper; $n = 3$) or EGFP-expressing fibroblasts and keratinocytes ($n = 4$). Magnified images of the boxed region are shown (white color indicates TRAP-positive osteoclasts; arrowheads). Scale bars, 250 μm. (B) Quantification of osteoclast surface per respective bone surface (Oc.S/BS) under the mass lesion. (C) Expression of RANKL in the mass lesion at low magnification (left) and high magnification (right) of the square region. Scale bars, 200 μm. Asterisks show weak staining in the epithelial layer, and arrowheads show strongly stained fibroblasts. Representative data from three mice are shown. Data are presented as means ± SD. *, $P < 0.05$ (Welch's *t* test).

mRNA expression of *Tnfsf11b* (encoding osteoprotegerin, a soluble decoy receptor for RANKL) was not affected throughout the experimental period.

We next examined whether these fibroblasts have the potential to induce osteoclastogenesis *in vitro*. Fibroblasts were first cocultured with keratinocytes, and then the keratinocyte-primed fibroblasts were sequentially cultured with bone marrow-derived monocyte-macrophage precursor cells (BMMs) from TRAP-tdTomato mice. Keratinocyte-primed fibroblasts induced TRAP-positive cells more effectively than fibroblasts cultured in the absence of keratinocytes (Fig. 4E). To examine the effect of RANKL deficiency in fibroblasts on osteoclast differentiation, *Tnfsf11*-deficient fibroblasts next were cocultured with keratinocytes, followed by culture with BMMs. Deletion of RANKL resulted in a dramatic decrease in formation of TRAP-positive multinucleated cells, indicating that fibroblast-derived RANKL induces osteoclast differentiation.

Soluble factors secreted by keratinocytes stimulate RANKL expression in ear pinna-derived fibroblasts in a MyD88-independent manner. The findings described above raised questions about the mechanism for the elevation of RANKL expression in keratinocyte-primed fibroblasts. Lipopolysaccharide (LPS) is known to induce RANKL expression in osteoblasts through stimulation of Toll-like receptor 4 (TLR4) (31). Ear pinna-derived fibroblasts also expressed *Tlr4* mRNA (Fig. 5A), and *Tnfsf11* mRNA expression was elevated after LPS stimulation (Fig. 5B). To examine whether keratinocytes enhance RANKL expression through TLR4 activation, we tested the effect of the knockout of myeloid differentiation primary response (*Myd88*), which is an adaptor molecule of TLR families (23). We isolated fibroblasts from ear pinnae of *Myd88* knockout mice. Knockout of *Myd88* almost completely abolished the effect of LPS on *Tnfsf11* mRNA expression (Fig. 5C). However, the induction of *Tnfsf11* mRNA expression by keratinocytes was not affected by knockout of *Myd88* (Fig. 5C). In contrast, LPS had no additive effect on keratinocyte supernatant-induced *Tnfsf11* expression (see Fig. S4A in the supplemental material). On the basis of these results, although keratinocytes increased the expression of *Tnfsf11* in a Myd88-independent manner, a common signaling molecule(s) likely is involved in LPS- or keratinocyte supernatant-induced *Tnfsf11* expression.

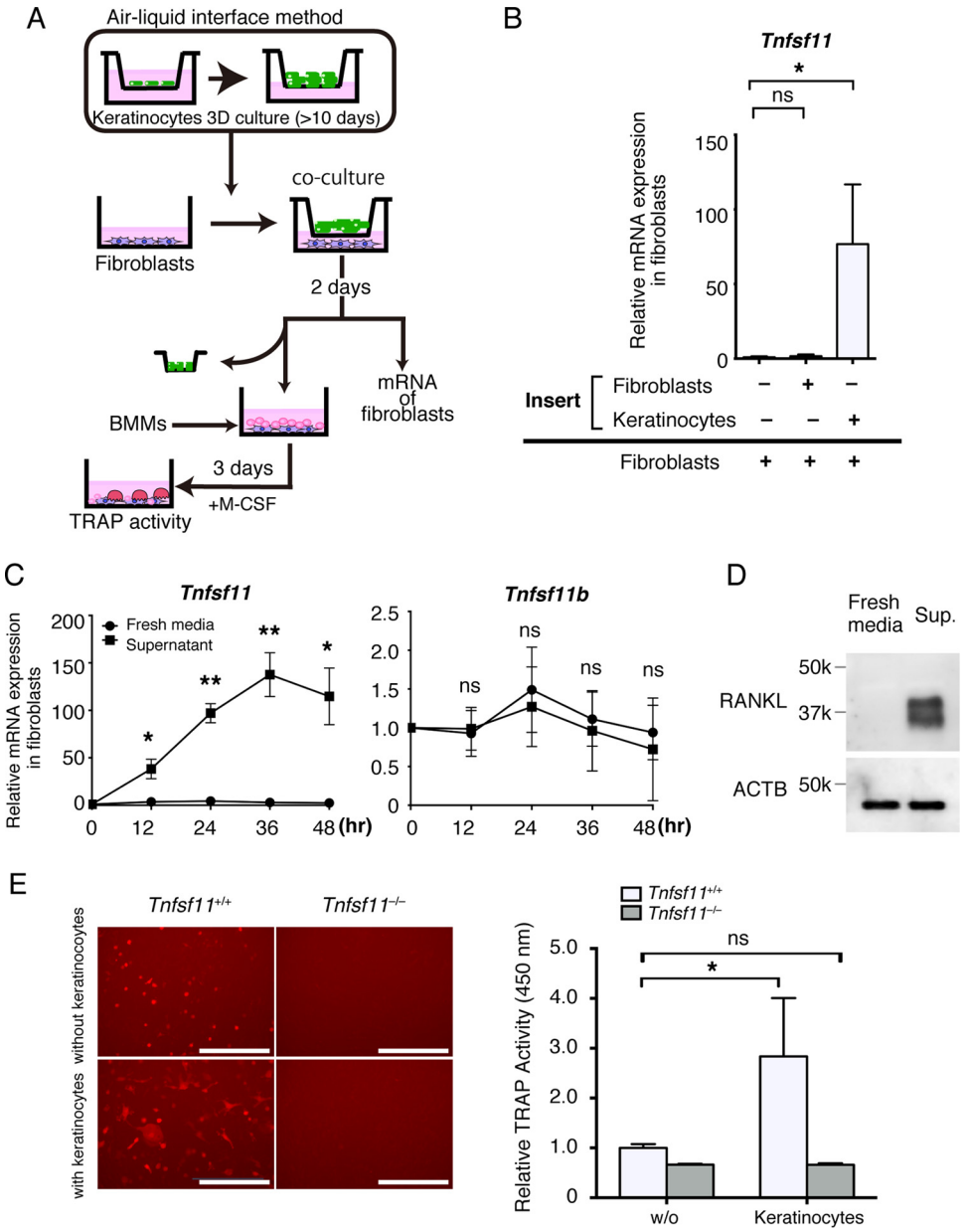

FIG 4 Soluble factors secreted by keratinocytes increase the expression of RANKL in fibroblasts. (A) Schematic of the method for coculture of ear pinna-derived fibroblasts, three-dimensional cultured keratinocytes, and bone marrow-derived monocyte-macrophage precursor cells (BMMs) as an *in vitro* model of epidermal cyst. (B) *Tnfsf11* expression in ear pinna-derived fibroblasts cocultured with inserts without cells, with fibroblasts, or with keratinocytes for 2 days. (C) Relative *Tnfsf11* and *Tnfsf11b* expression in ear pinna-derived fibroblasts cultured in fresh media and supernatant from keratinocyte culture for the indicated time periods, measured by RT-qPCR analysis. (D) RANKL expression in ear pinna-derived fibroblasts cultured in fresh medium or supernatant (Sup.) from keratinocyte culture for 2 days as determined by immunoblot analysis using anti-RANKL antibody and anti-ACTB antibodies. (E, left) Representative images of tdTomato-positive cells showing osteoclast differentiation of BMMs cultured with fibroblasts obtained from *Tnfsf11*$^{+/+}$ mice or *Tnfsf11*$^{-/-}$ mice after coculture with transwell culture inserts lacking cells or with keratinocytes. (Right) Relative TRAP activity was determined by TRAP solution assay. w/o, without. Scale bars, 250 μm. Data are presented as means ± SD. *, $P < 0.05$; **$P < 0.01$; ns, not significant (determined by Kruskal-Wallis test [B], Welch's *t* test [C], and two-way ANOVA [E]).

Through the screening of cytokines secreted from keratinocytes with the use of an antibody array recognizing 308 different murine cytokines, we found that 18 cytokines were increased more than 3-fold in keratinocyte culture supernatant compared to the level in fresh media (Table 2). Among them, galectin-3 (Gal-3; encoded by the *Lgals3* gene), urokinase (uPA; encoded by the *Plau* gene), secretory leukocyte protease inhibitor (SLPI; encoded by the *Slpi* gene), and vascular endothelial growth factor (VEGF; encoded by the *Vegfa* gene) have been reported to be expressed in cholesteatoma (32–35). We confirmed the mRNA expression of these genes and several top-ranked genes from the results of the cytokine array (see Fig. S4B in the supplemental material). We focused on galectin-3, Cxcl-1, Cxcl-16, and VEGF, which were highly expressed in keratinocytes. However, although we exam-

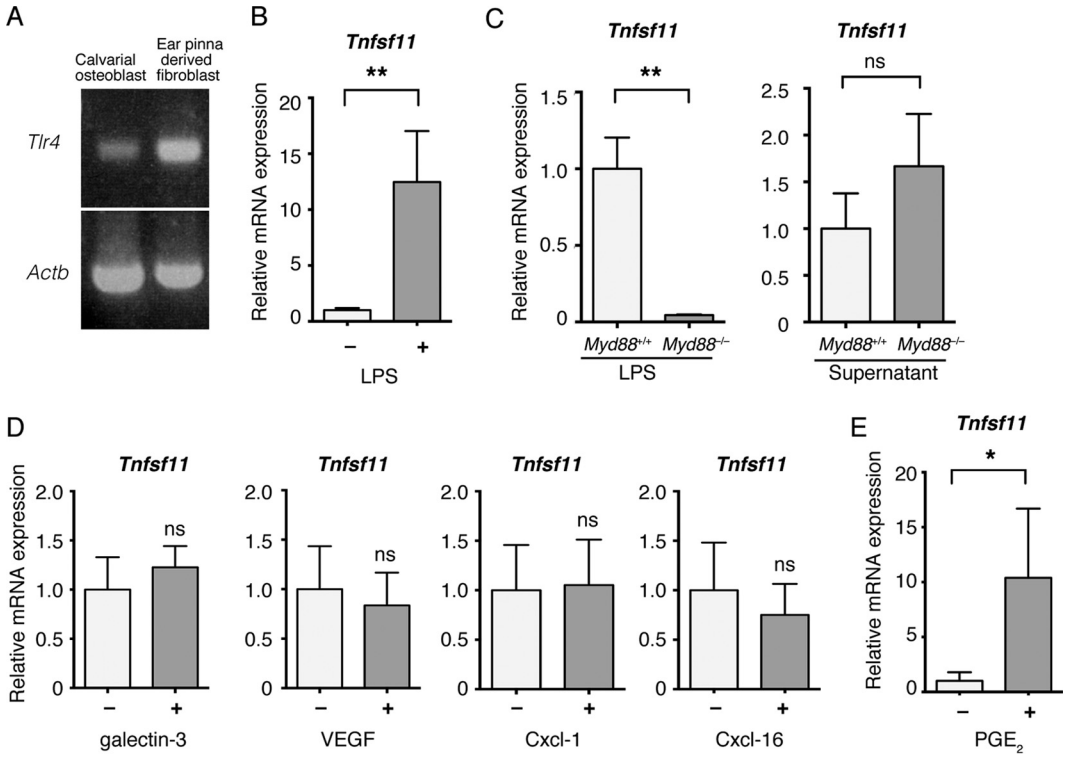

FIG 5 Soluble factors secreted by keratinocytes stimulate the expression of RANKL in ear pinna-derived fibroblasts in a MyD88-independent manner. (A) *Tlr4* mRNA expression in calvarial osteoblasts and ear pinna-derived fibroblasts. (B) Effect of LPS on *Tnfsf11* mRNA expression in ear pinna-derived fibroblasts, measured by RT-qPCR analysis. (C) Effect of *Myd88* knockout on *Tnfsf11* mRNA expression in response to LPS (left) and supernatant from keratinocyte culture (right), measured by RT-qPCR analysis. (D) Effects of recombinant mouse galectin-3, VEGF, Cxcl-1, and Cxcl-16 proteins on *Tnfsf11* mRNA expression in ear pinna-derived fibroblasts, measured by RT-qPCR analysis. (E) Effect of PGE_2 on *Tnfsf11* mRNA expression in ear pinna-derived fibroblasts, measured by RT-qPCR analysis. Data are presented as means ± SD. *, $P < 0.05$; **, $P < 0.01$; ns, not significant (determined by ratio paired *t* test [B and E] and Welch's *t* test [C and D].

ined the effect of these molecules on *Tnfsf11* expression on fibroblasts with these recombinant proteins, they did not affect *Tnfsf11* expression (Fig. 5D). We next tested the effect of prostaglandin E_2 (PGE_2) on *Tnfsf11* expression in fibroblasts, since it is known as a key inducer of *Tnfsf11* expression in osteoblasts (36, 37). PGE_2 significantly upregulated *Tnfsf11* expression in ear pinna-derived fibroblasts (Fig. 5E), suggesting PGE_2 is a candidate for a RANKL inducer.

DISCUSSION

The cross talk between the skeletal and immune systems has long been studied. In most bone destructive diseases, including autoimmune diseases such as RA, bone-resorbing osteoclasts are activated via the RANK-RANKL axis. It has become clear that synoviocytes and T or B cells function as the source of RANKL in pathological states (9–11). However, the underlying mechanisms for bone destruction in cholesteatoma remain to be elucidated. Currently, it is controversial whether osteoclasts are the cause of bone destruction in cholesteatoma (38). Some reports have shown that osteoclasts accumulate on the bone surface in cholesteatoma (39–41; unpublished data). A number of studies have addressed the fact that RANKL is expressed in cholesteatoma clinical samples, and meta-analysis data showed that higher levels of RANKL are prominent features in middle ear cholesteatoma (42). However, the localization of RANKL is also controversial. Some have reported it is expressed in the epithelial layer (43), others showed it was expressed in the subepithelial layer, including infiltrated inflammatory cells (44), and still others found both the epithelial layer and subepithelial layer (45, 46) expressed RANKL in cholesteatoma. What makes these problems difficult to solve is partially that cholesteatoma is usually removed piece by piece, and the obtained clinical samples are very small. Accordingly, animal experimentation is essential to the elucidation of the pathogenesis of cholesteatoma.

To date, some animal models of cholesteatoma have been reported. The Mongolian gerbil develops spontaneous cholesteatoma (47–49), which is known to cause bone resorption and is used as a cholesteatoma model. Additionally, chinchillas and guinea pigs have been used as cholesteatoma models (50, 51). Recently, it was also reported that overexpression of KGF by electroporation of KGF cDNA leads to cholesteatoma formation in rats (52). In that study, the authors reported that repeated introductions of KGF for 2 months led to bone resorption. However, most of these animal models involved relatively large rodents. For molecular analysis of pathogenesis, the mouse is a more suitable animal model due to its uniform genetic background and its facility for genetic modification. In this study, we succeeded in establishing a mouse model by reconstructing the epidermal cyst-like tissue composed of keratinocytes and fibroblasts. In this model, we detected osteoclastogenesis on the bone surface; however, bone destruction was not detected. We could not examine the long-term effect of cysts on bone destruction because cysts grad-

TABLE 2 Cytokines increased more than 3-fold in keratinocyte culture supernatant compared to levels in fresh medium

Cytokine	Net intensity		Ratio
	Fresh medium	Keratinocyte supernatant	
Progranulin	653.639855	46,431.40121	71.03514398
Progranulin	705.692483	46,733.85061	66.22410148
TGF-β RII	1,464.800341	42,457.89185	28.98544645
KC	540.782057	15,460.02704	28.58827662
Urokinase	952.411505	21,742.83461	22.82924397
SLPI	2,756.440908	55,488.95506	20.13065286
SLPI	2,798.336582	54,477.45013	19.46779758
KC	823.727044	15,790.09523	19.16908683
VEGF	1,142.112759	18,847.23739	16.50208111
TGF-β RII	2,433.635287	39,960.2164	16.41996918
VEGF	1,202.464262	19,266.72335	16.02269935
Galectin-3	5,446.539514	59,189.22117	10.86730777
IGFBP-1	4,483.21684	46,134.77865	10.29055259
Galectin-3	5,688.203579	56,892.80468	10.0018932
IL-9	4,406.821408	44,031.72739	9.991720406
IL-9	4,398.046924	43,181.95986	9.818440003
IGFBP-1	5,081.677559	43,327.84467	8.526287662
IL-17RD	1,687.691979	13,979.29744	8.283085784
TNF RI/TNFRSF1A	1,637.094572	12,373.19429	7.55802047
TNF RI/TNFRSF1A	1,721.384375	12,875.96204	7.480004017
IGFBP-3	4,226.882388	27,981.13167	6.6198037
Dtk	3,230.443095	20,631.52063	6.386591567
IL-17RD	1578.377106	10,047.68026	6.365829954
IGFBP-3	4140.794435	23,198.28048	5.602374338
CXCL16	5806.469286	29,251.37525	5.037721516
IL-17 BR	3107.405808	15,032.52332	4.837644082
G-CSF	5297.390889	24,369.00957	4.600190938
IL-17 BR	3150.290978	13,969.29238	4.434286381
CXCL16	5837.528539	23,715.76882	4.062638608
G-CSF	5619.723968	22,315.80974	3.97097969
Dtk	3361.140557	12,999.2189	3.867502319
IGFBP-2	5438.47084	18,701.63065	3.438766373
Urokinase	6937.981477	22,537.89271	3.248479804
IL-15 Rα	3938.349311	12,372.11284	3.141446291

ually became smaller after 1 week. Some factors and/or cells seem to be needed for the maintenance of cysts.

The intercellular communication between keratinocytes and fibroblasts has been an area of focus, both for physiological states such as normal skin and for pathological states such as psoriasis or cholesteatoma. Using our mouse model, we demonstrated that their cross talk also is involved in the regulation of the expression of RANKL. Previous studies have shown that keratinocytes express RANKL especially when they were irradiated by ultraviolet light (53, 54). However, our data revealed that RANKL was scarcely expressed in keratinocytes of epidermal cyst-like tissue. Instead, fibroblasts stimulated by keratinocytes highly expressed RANKL. The upstream signaling pathways of RANKL are not fully understood. LPS, IL-1α, IL-6, parathyroid hormone (PTH), 1α,25-dihydroxyvitamin D_3 [1α,25$(OH)_2D_3$], and PGE_2 are known to be involved in the expression of RANKL in osteoblasts. LPS and IL-1α activate the expression of RANKL through calcium/protein kinase C signals via MyD88 (55). Although IL-1 is well-known to be produced by keratinocytes, RANKL induction by keratinocyte supernatant was not affected by knockout of *Myd88*, indicating IL-1 is not involved in this reaction. Our cytokine array analysis has produced 18 candidates for RANKL inducers secreted by keratinocytes. Previous reports showed that galectin-3, urokinase, SLPI, and VEGF were expressed in cholesteatoma (32–35). In our experiment, *Lgals3* and *Vegfa* mRNA expression was relatively higher in keratinocytes than in fibroblasts. Even in clinical samples, immunohistochemistry has demonstrated that the expression of galectin-3 is higher in the epithelial layer than in subepithelial connective tissue (56). Galectin-3 is a positive regulator of IL-6 in synoviocytes or fibroblasts (57, 58). Since IL-6 induces RANKL in osteoblasts (59, 60), it is conceivable that keratinocyte-derived galectin-3 could regulate RANKL expression in fibroblasts through the induction of IL-6. VEGF also seems to be closely associated with bone metabolism, as it has been reported to regulate osteoclast survival and mobility as well as RANKL expression in an osteoblastic cell line (61). However, neither galectin-3 nor VEGF had direct effects on RANKL expression in fibroblasts. In contrast, we confirmed that PGE_2 has a significant effect on RANKL expression in ear pinna-derived fibroblasts. PGE_2 can be produced in a variety of cell types, including fibroblasts and keratinocytes (37, 62). Therefore, PGE_2 is a potential candidate for a RANKL inducer through the intracellular communication between keratinocytes and fibroblasts. RANKL is known to be expressed in several normal tissues, including thymus and mammary gland (24, 63, 64). In addition, we found RANKL was expressed in subepithelial connective tissue of normal skin and ear pinna. In these tissues, hypodermal tissue and muscle separate RANKL-expressing dermis from bone surfaces. This may hamper osteoclast formation.

Currently, the only therapy for cholesteatoma is surgical removal; however, there are some drawbacks to this treatment. Complications of surgery, such as deafness, dizziness, and facial nerve palsy, can sometimes occur (65–67). Furthermore, it sometimes makes it difficult to identify recurrent or residual cholesteatoma (68, 69). Preventing secondary infection by aspiration of debris makes cholesteatoma less aggressive and decreases complications; however, regular treatment is needed throughout life. Therefore, a more definitive nonsurgical remedy is required. Suppression of osteoclastogenesis or osteoclast function has already been identified as a therapeutic target for bone diseases such as RA or osteoporosis (29, 70, 71). Our findings unveiled that intercellular communication between keratinocytes and fibroblasts is involved in the differentiation of osteoclasts, which may provide the molecular basis for a new therapeutic strategy for cholesteatoma-induced bone destruction.

ACKNOWLEDGMENTS

We thank Junichi Kikuta, Mika Terao, Noriko Takegahara, and Hiroki Mizuno for help and discussions, Kiyoshi Takeda for providing *Myd88* knockout mice, Nobuyuki Udagawa for providing *Tnfsf11* knockout mice, and Junichi Miyazaki for providing the CAG-Cre mice.

This work was supported by a grant-in-aid for scientific research (A) from the Japan Society for the Promotion of Science (JSPS) (25253070 to M.I.), grant-in-aid for young scientists (B) from JSPS (70636480 to Y.I.), grant-in-aid for scientific research on innovative areas from the Ministry of Education, Culture, Sports, Science and Technology (MEXT) (15H01405 to K.N.), grant-in-aid for young scientists (A) from the JSPS (26713010 to K.N.), grants from the Takeda Science Foundation (to M.I. and K.N.), the Astellas Foundation for Research on Metabolic Disorders (to K.N.), the Kanae Foundation for the Promotion of Medical Science (to M.I. and K.N.), the LOTTE Foundation (to K.N.), the Research Founda-

tion for Opto-Science and Technology, the Life Science Foundation of Japan (to K.N.), and the Kishimoto Foundation (to K.N.).

FUNDING INFORMATION

This work, including the efforts of Yoriko Iwamoto, was funded by Japan Society for the Promotion of Science (JSPS) (70636480). This work, including the efforts of Keizo Nishikawa, was funded by MEXT (15H01405). This work, including the efforts of Keizo Nishikawa, was funded by Japan Society for the Promotion of Science (JSPS) (26713010). This work, including the efforts of Masaru Ishii, was funded by Japan Society for the Promotion of Science (JSPS) (25253070). This work, including the efforts of Keizo Nishikawa and Masaru Ishii, was funded by Takeda Science Foundation. This work, including the efforts of Keizo Nishikawa, was funded by Astellas Foundation for Research on Metabolic Disorders.

The funders had no role in study design, data collection and interpretation, or the decision to submit the work for publication.

REFERENCES

1. **Ishii M, Egen JG, Klauschen F, Meier-Schellersheim M, Saeki Y, Vacher J, Proia RL, Germain RN.** 2009. Sphingosine-1-phosphate mobilizes osteoclast precursors and regulates bone homeostasis. Nature **458:**524–528. http://dx.doi.org/10.1038/nature07713.
2. **Ishii M, Kikuta J, Shimazu Y, Meier-Schellersheim M, Germain RN.** 2010. Chemorepulsion by blood S1P regulates osteoclast precursor mobilization and bone remodeling in vivo. J Exp Med **207:**2793–2798. http://dx.doi.org/10.1084/jem.20101474.
3. **Teitelbaum SL, Ross FP.** 2003. Genetic regulation of osteoclast development and function. Nat Rev Genet **4:**638–649. http://dx.doi.org/10.1038/nrg1122.
4. **Maeda K, Kobayashi Y, Udagawa N, Uehara S, Ishihara A, Mizoguchi T, Kikuchi Y, Takada I, Kato S, Kani S, Nishita M, Marumo K, Martin TJ, Minami Y, Takahashi N.** 2012. Wnt5a-Ror2 signaling between osteoblast-lineage cells and osteoclast precursors enhances osteoclastogenesis. Nat Med **18:**405–412. http://dx.doi.org/10.1038/nm.2653.
5. **Kim H, Kim T, Jeong B-C, Cho I-T, Han D, Takegahara N, Negishi-Koga T, Takayanagi H, Lee JH, Sul J-Y, Prasad V, Lee SH, Choi Y.** 2013. Tmem64 modulates calcium signaling during RANKL-mediated osteoclast differentiation. Cell Metab **17:**249–260. http://dx.doi.org/10.1016/j.cmet.2013.01.002.
6. **Lacey D, Timms E, Tan H-L, Kelley M, Dunstan C, Burgess T, Elliott R, Colombero A, Elliott G, Scully S, Hsu H, Sullivan J, Hawkins N, Davy E, Capparelli C, Eli A, Qian Y-X, Kaufman S, Sarosi I, Shalhoub V, Senaldi G, Guo J, Delaney J, Boyle W.** 1998. Osteoprotegerin ligand is a cytokine that regulates osteoclast differentiation and activation. Cell **93:**165–176. http://dx.doi.org/10.1016/S0092-8674(00)81569-X.
7. **Fuller K, Wong B, Fox S, Choi Y, Chambers TJ.** 1998. TRANCE is necessary and sufficient for osteoblast-mediated activation of bone resorption in osteoclasts. J Exp Med **188:**997–1001. http://dx.doi.org/10.1084/jem.188.5.997.
8. **Nakashima T, Hayashi M, Fukunaga T, Kurata K, Oh-Hora M, Feng JQ, Bonewald LF, Kodama T, Wutz A, Wagner EF, Penninger JM, Takayanagi H.** 2011. Evidence for osteocyte regulation of bone homeostasis through RANKL expression. Nat Med **17:**1231–1234. http://dx.doi.org/10.1038/nm.2452.
9. **Takayanagi H, Iizuka H, Juji T, Nakagawa T, Yamamoto A, Miyazaki T, Koshihara Y, Oda H, Nakamura K, Tanaka S.** 2000. Involvement of receptor activator of nuclear factor kappaB ligand/osteoclast differentiation factor in osteoclastogenesis from synoviocytes in rheumatoid arthritis. Arthritis Rheum **43:**259–269. http://dx.doi.org/10.1002/1529-0131(200002)43:2<259::AID-ANR4>3.0.CO;2-W.
10. **Kong YY, Feige U, Sarosi I, Bolon B, Tafuri A, Morony S, Capparelli C, Li J, Elliott R, McCabe S, Wong T, Campagnuolo G, Moran E, Bogoch ER, Van G, Nguyen LT, Ohashi PS, Lacey DL, Fish E, Boyle WJ, Penninger JM.** 1999. Activated T cells regulate bone loss and joint destruction in adjuvant arthritis through osteoprotegerin ligand. Nature **402:**304–309. http://dx.doi.org/10.1038/46303.
11. **Kawai T, Matsuyama T, Hosokawa Y, Makihira S, Seki M, Karimbux NY, Goncalves RB, Valverde P, Dibart S, Li Y-P, Miranda LA, Ernst CWO, Izumi Y, Taubman MA.** 2006. B and T lymphocytes are the primary sources of RANKL in the bone resorptive lesion of periodontal disease. Am J Pathol **169:**987–998. http://dx.doi.org/10.2353/ajpath.2006.060180.
12. **Takayanagi H.** 2007. Osteoimmunology: shared mechanisms and crosstalk between the immune and bone systems. Nat Rev Immunol **7:**292–304. http://dx.doi.org/10.1038/nri2062.
13. **Sato K, Suematsu A, Okamoto K, Yamaguchi A, Morishita Y, Kadono Y, Tanaka S, Kodama T, Akira S, Iwakura Y, Cua DJ, Takayanagi H.** 2006. Th17 functions as an osteoclastogenic helper T cell subset that links T cell activation and bone destruction. J Exp Med **203:**2673–2682. http://dx.doi.org/10.1084/jem.20061775.
14. **Banco B, Grieco V, Di Giancamillo M, Greci V, Travetti O, Martino P, Mortellaro CM, Giudice C.** 2014. Canine aural cholesteatoma: a histological and immunohistochemical study. Vet J **200:**440–445. http://dx.doi.org/10.1016/j.tvjl.2014.03.018.
15. **Beales P.** 1978. Pathogenesis of attic cholesteatomas. J R Soc Med **71:**707–708.
16. **Dornelles C, da Costa SS, Meurer L, Schweiger C.** 2005. Some considerations about acquired adult and pediatric cholesteatomas. Rev Bras Otorrinolaringol **71:**536–546. http://dx.doi.org/10.1590/S0034-72992005000400023.
17. **Chole RA.** 1997. The molecular biology of bone resorption due to chronic otitis media. Ann N Y Acad Sci **830:**95–109. http://dx.doi.org/10.1111/j.1749-6632.1997.tb51882.x.
18. **Kuo C-L.** 2015. Etiopathogenesis of acquired cholesteatoma: prominent theories and recent advances in biomolecular research. Laryngoscope **125:**234–240. http://dx.doi.org/10.1002/lary.24890.
19. **Yoshikawa M, Kojima H, Wada K, Tsukidate T, Okada N, Saito H, Moriyama H.** 2006. Identification of specific gene expression profiles in fibroblasts derived from middle ear cholesteatoma. Arch Otolaryngol Head Neck Surg **132:**734–742. http://dx.doi.org/10.1001/archotol.132.7.734.
20. **Yamamoto-Fukuda T, Aoki D, Hishikawa Y, Kobayashi T, Takahashi H, Koji T.** 2003. Possible involvement of keratinocyte growth factor and its receptor in enhanced epithelial-cell proliferation and acquired recurrence of middle-ear cholesteatoma. Lab Investig **83:**123–136. http://dx.doi.org/10.1097/01.LAB.0000050763.64145.CB.
21. **Yoshikawa M, Kojima H, Yaguchi Y, Okada N, Saito H, Moriyama H.** 2013. Cholesteatoma fibroblasts promote epithelial cell proliferation through overexpression of epiregulin. PLoS One **8:**e66725. http://dx.doi.org/10.1371/journal.pone.0066725.
22. **Kikuta J, Wada Y, Kowada T, Wang Z, Sun-Wada G-H, Nishiyama I, Mizukami S, Maiya N, Yasuda H, Kumanogoh A, Kikuchi K, Germain RN, Ishii M.** 2013. Dynamic visualization of RANKL and Th17-mediated osteoclast function. J Clin Investig **123:**866–873.
23. **Adachi O, Kawai T, Takeda K, Matsumoto M, Tsutsui H, Sakagami M, Nakanishi K, Akira S.** 1998. Targeted disruption of the MyD88 gene results in loss of IL-1- and IL-18-mediated function. Immunity **9:**143–150. http://dx.doi.org/10.1016/S1074-7613(00)80596-8.
24. **Kong YY, Yoshida H, Sarosi I, Tan HL, Timms E, Capparelli C, Morony S, Oliveira-dos-Santos AJ, Van G, Itie A, Khoo W, Wakeham A, Dunstan CR, Lacey DL, Mak TW, Boyle WJ, Penninger JM.** 1999. OPGL is a key regulator of osteoclastogenesis, lymphocyte development and lymph-node organogenesis. Nature **397:**315–323. http://dx.doi.org/10.1038/16852.
25. **Sakai K, Miyazaki J.** 1997. A transgenic mouse line that retains Cre recombinase activity in mature oocytes irrespective of the cre transgene transmission. Biochem Biophys Res Commun **237:**318–324. http://dx.doi.org/10.1006/bbrc.1997.7111.
26. **Ogata N, Chikazu D, Kubota N, Terauchi Y, Tobe K, Azuma Y, Ohta T, Kadowaki T, Nakamura K, Kawaguchi H.** 2000. Insulin receptor substrate-1 in osteoblast is indispensable for maintaining bone turnover. J Clin Investig **105:**935–943. http://dx.doi.org/10.1172/JCI9017.
27. **Nishikawa K, Nakashima T, Hayashi M, Fukunaga T, Kato S, Kodama T, Takahashi S, Calame K, Takayanagi H.** 2010. Blimp1-mediated repression of negative regulators is required for osteoclast differentiation. Proc Natl Acad Sci U S A **107:**3117–3122. http://dx.doi.org/10.1073/pnas.0912779107.
28. **Nishikawa K.** 2010. Maf promotes osteoblast differentiation in mice by mediating the age-related switch in mesenchymal cell differentiation. J Clin Investig **120:**3455–3465. http://dx.doi.org/10.1172/JCI42528.
29. **Nishikawa K, Iwamoto Y, Kobayashi Y, Katsuoka F, Kawaguchi S, Tsujita T, Nakamura T, Kato S, Yamamoto M, Takayanagi H, Ishii M.** 2015. DNA methyltransferase 3a regulates osteoclast differentiation by

coupling to an S-adenosylmethionine-producing metabolic pathway. Nat Med **21:**281–287.
30. **Miyamoto T, Arai F, Ohneda O, Takagi K, Anderson DM, Suda T.** 2000. An adherent condition is required for formation of multinuclear osteoclasts in the presence of macrophage colony-stimulating factor and receptor activator of nuclear factor kappa B ligand. Blood **96:**4335–4343.
31. **Zou W, Bar-Shavit Z.** 2002. Dual modulation of osteoclast differentiation by lipopolysaccharide. J Bone Miner Res **17:**1211–1218. http://dx.doi.org/10.1359/jbmr.2002.17.7.1211.
32. **Nakamura M, Yamashiro Y, Nakahodo K, Sunagawa M, Huang GW, Kosugi T, Morimitsu T.** 1995. Plasminogen activators in tissue extract of aural cholesteatoma. Laryngoscope **105:**305–310. http://dx.doi.org/10.1288/00005537-199503000-00015.
33. **Naim R, Riedel F, Hormann K.** 2003. Expression of vascular endothelial growth factor in external auditory canal cholesteatoma. Int J Mol Med **11:**555–558.
34. **Vander Ghinst M, Remmelink M, Mansbach A-L, Hassid S, Choufani G.** 2012. Galectin-1, -3, -7 expressions in congenital and acquired pediatric cholesteatomas compared to external auditory canal skin. Clin Exp Otorhinolaryngol **5:**62–67. http://dx.doi.org/10.3342/ceo.2012.5.2.62.
35. **Lee J-K, Chae S-W, Cho J-G, Lee H-M, Hwang S-J, Jung H-H.** 2006. Expression of secretory leukocyte protease inhibitor in middle ear cholesteatoma. Eur Arch Otorhinolaryngol **263:**1077–1081. http://dx.doi.org/10.1007/s00405-006-0126-7.
36. **Udagawa N, Takahashi N, Jimi E, Matsuzaki K, Tsurukai T, Itoh K, Nakagawa N, Yasuda H, Goto M, Tsuda E, Higashio K, Gillespie M, Martin T, Suda T.** 1999. Osteoblasts/stromal cells stimulate osteoclast activation through expression of osteoclast differentiation factor/RANKL but not macrophage colony-stimulating factor. Bone **25:**517–523. http://dx.doi.org/10.1016/S8756-3282(99)00210-0.
37. **Pentland AP, Mahoney MG.** 1990. Keratinocyte prostaglandin synthesis is enhanced by IL-1. J Investig Dermatol **94:**43–46. http://dx.doi.org/10.1111/1523-1747.ep12873337.
38. **Koizumi H, Suzuki H, Ikezaki S, Ohbuchi T, Hashida K, Sakai A.** 2015. Osteoclasts are not activated in middle ear cholesteatoma. J Bone Miner Metab **34:**193–200.
39. **Chole RA.** 1988. Osteoclasts in chronic otitis media, cholesteatoma, and otosclerosis. Ann Otol Rhinol Laryngol **97:**661–666. http://dx.doi.org/10.1177/000348948809700615.
40. **Chole RA.** 1984. Cellular and subcellular events of bone resorption in human and experimental cholesteatoma: the role of osteoclasts. Laryngoscope **94:**76–95. http://dx.doi.org/10.1002/lary.5540940117.
41. **Uno Y, Saito R.** 1995. Bone resorption in human cholesteatoma: morphological study with scanning electron microscopy. Ann Otol Rhinol Laryngol **104:**463–468. http://dx.doi.org/10.1177/000348949510400609.
42. **Chen A-P, Wang B, Zhong F, Song G-Z, Song H-F, Yu K, Wang H-B, Jiang Z-H.** 2015. Expression levels of receptor activator of nuclear factor-κB ligand and osteoprotegerin are associated with middle ear cholesteatoma risk. Acta Otolaryngol **135:**655–666. http://dx.doi.org/10.3109/00016489.2015.1011789.
43. **Miyasato M, Takeno S, Hirakawa K.** 2013. Expression of RANKL and proliferation abilities of cultured human middle ear cholesteatoma epithelial cells. Hiroshima J Med Sci **62:**1–6.
44. **Hamzei M, Ventriglia G, Hagnia M, Antonopolous A, Bernal-Sprekelsen M, Dazert S, Hildmann H, Sudhoff H.** 2003. Osteoclast stimulating and differentiating factors in human cholesteatoma. Laryngoscope **113:**436–442. http://dx.doi.org/10.1097/00005537-200303000-00009.
45. **Jeong J-H, Park C-W, Tae K, Lee S-H, Shin D-H, Kim K-R, Park Y-W.** 2006. Expression of RANKL and OPG in middle ear cholesteatoma tissue. Laryngoscope **116:**1180–1184. http://dx.doi.org/10.1097/01.mlg.0000224345.59291.da.
46. **Kuczkowski J, Sakowicz-Burkiewicz M, Iżycka-Świeszewska E.** 2010. Expression of the receptor activator for nuclear factor-κB ligand and osteoprotegerin in chronic otitis media. Am J Otolaryngol **31:**404–409. http://dx.doi.org/10.1016/j.amjoto.2009.06.004.
47. **Henry KR, Chole RA, McGinn MD.** 1983. Age-related increase of spontaneous aural cholesteatoma in the Mongolian gerbil. Arch Otolaryngol **109:**19–21. http://dx.doi.org/10.1001/archotol.1983.00800150023004.
48. **McGinn MD, Chole RA, Henry KR.** 1982. Cholesteatoma. Experimental induction in the Mongolian gerbil, Meriones unguiculaus. Acta Otolaryngol **93:**61–67.
49. **Chole RA, Henry KR, McGinn MD.** 1981. Cholesteatoma: spontaneous occurrence in the Mongolian gerbil Meriones unguiculatis. Am J Otol **2:**204–210.
50. **Hinohira Y, Gyo K, Yanagihara N.** 1994. Experimental cholesteatomas arising from autologous free skin grafting in the middle ear cavity. Acta Otolaryngol **114:**533–538. http://dx.doi.org/10.3109/00016489409126099.
51. **Jove MA, Vassalli L, Raslan W, Applebaum EL.** 1990. The effect of isotretinoin on propylene glycol-induced cholesteatoma in chinchilla middle ears. Am J Otolaryngol **11:**5–9. http://dx.doi.org/10.1016/0196-0709(90)90163-P.
52. **Yamamoto-Fukuda T, Akiyama N, Shibata Y, Takahashi H, Ikeda T, Koji T.** 2015. In vivo over-expression of KGF mimic human middle ear cholesteatoma. Eur Arch Otorhinolaryngol **272:**2689–2696. http://dx.doi.org/10.1007/s00405-014-3237-6.
53. **Loser K, Mehling A, Loeser S, Apelt J, Kuhn A, Grabbe S, Schwarz T, Penninger JM, Beissert S.** 2006. Epidermal RANKL controls regulatory T-cell numbers via activation of dendritic cells. Nat Med **12:**1372–1379.
54. **Soontrapa K, Honda T, Sakata D, Yao C, Hirata T, Hori S, Matsuoka T, Kita Y, Shimizu T, Kabashima K, Narumiya S.** 2011. Prostaglandin E2-prostaglandin E receptor subtype 4 (EP4) signaling mediates UV irradiation-induced systemic immunosuppression. Proc Natl Acad Sci U S A **108:**6668–6673. http://dx.doi.org/10.1073/pnas.1018625108.
55. **Sato N, Takahashi N, Suda K, Nakamura M, Yamaki M, Ninomiya T, Kobayashi Y, Takada H, Shibata K, Yamamoto M, Takeda K, Akira S, Noguchi T, Udagawa N.** 2004. MyD88 but not TRIF is essential for osteoclastogenesis induced by lipopolysaccharide, diacyl lipopeptide, and IL-1alpha. J Exp Med **200:**601–611. http://dx.doi.org/10.1084/jem.20040689.
56. **Sheikholeslam-Zadeh R, Decaestecker C, Delbrouck C, Danguy A, Salmon I, Zick Y, Kaltner H, Hassid S, Gabius HJ, Kiss R, Choufani G.** 2001. The levels of expression of galectin-3, but not of galectin-1 and galectin-8, correlate with apoptosis in human cholesteatomas. Laryngoscope **111:**1042–1047. http://dx.doi.org/10.1097/00005537-200106000-00020.
57. **Filer A, Bik M, Parsonage GN, Fitton J, Trebilcock E, Howlett K, Cook M, Raza K, Simmons DL, Thomas AMC, Salmon M, Scheel-Toellner D, Lord JM, Rabinovich GA, Buckley CD.** 2009. Galectin 3 induces a distinctive pattern of cytokine and chemokine production in rheumatoid synovial fibroblasts via selective signaling pathways. Arthritis Rheum **60:**1604–1614. http://dx.doi.org/10.1002/art.24574.
58. **Arad U, Madar-Balakirski N, Angel-Korman A, Amir S, Tzadok S, Segal O, Menachem A, Gold A, Elkayam O, Caspi D.** 2015. Galectin-3 is a sensor-regulator of toll-like receptor pathways in synovial fibroblasts. Cytokine **73:**30–35. http://dx.doi.org/10.1016/j.cyto.2015.01.016.
59. **Palmqvist P, Persson E, Conaway HH, Lerner UH.** 2002. IL-6, leukemia inhibitory factor, and oncostatin m stimulate bone resorption and regulate the expression of receptor activator of NF-κB ligand, osteoprotegerin, and receptor activator of NF-κB in mouse calvariae. J Immunol **169:**3353–3362. http://dx.doi.org/10.4049/jimmunol.169.6.3353.
60. **O'Brien CA, Gubrij I, Lin S-C, Saylors RL, Manolagas SC.** 1999. STAT3 activation in stromal/osteoblastic cells is required for induction of the receptor activator of NF-κB ligand and stimulation of osteoclastogenesis by gp130-utilizing cytokines or interleukin-1 but not 1,25-dihydroxyvitamin D3 or parathyroid hormone. J Biol Chem **274:**19301–19308. http://dx.doi.org/10.1074/jbc.274.27.19301.
61. **Nakai T, Yoshimura Y, Deyama Y, Suzuki K, Iida J.** 2009. Mechanical stress up-regulates RANKL expression via the VEGF autocrine pathway in osteoblastic MC3T3-E1 cells. Mol Med Rep **2:**229–234.
62. **Pentland AP, Needleman P.** 1986. Modulation of keratinocyte proliferation in vitro by endogenous prostaglandin synthesis. J Clin Investig **77:**246–251. http://dx.doi.org/10.1172/JCI112283.
63. **Fata JE, Kong Y-Y, Li J, Sasaki T, Irie-Sasaki J, Moorehead RA, Elliott R, Scully S, Voura EB, Lacey DL, Boyle WJ, Khokha R, Penninger JM.** 2000. The osteoclast differentiation factor osteoprotegerin-ligand is essential for mammary gland development. Cell **103:**41–50. http://dx.doi.org/10.1016/S0092-8674(00)00103-3.
64. **Ikeda T, Kasai M, Utsuyama M, Hirokawa K.** 2001. Determination of three isoforms of the receptor activator of nuclear factor-kappaB ligand and their differential expression in bone and thymus. Endocrinology **142:**1419–1426. http://dx.doi.org/10.1210/endo.142.4.8070.
65. **Sengupta A, Anwar T, Ghosh D, Basak B.** 2010. A study of surgical management of chronic suppurative otitis media with cholesteatoma and

its outcome. Indian J Otolaryngol Head Neck Surg **62:**171–176. http://dx.doi.org/10.1007/s12070-010-0043-3.
66. **Garap JP, Dubey SP.** 2001. Canal-down mastoidectomy: experience in 81 cases. Otol Neurotol **22:**451–456. http://dx.doi.org/10.1097/00129492-200107000-00006.
67. **Green JD, Shelton C, Brackmann DE.** 1994. Iatrogenic facial nerve injury during otologic surgery. Laryngoscope **104:**922–926.
68. **Edfeldt L, Strömbäck K, Kinnefors A, Rask-Andersen H.** 2013. Surgical treatment of adult cholesteatoma: long-term follow-up using total reconstruction procedure without staging. Acta Otolaryngol **133:**28–34.
69. **Tomlin J, Chang D, McCutcheon B, Harris J.** 2013. Surgical technique and recurrence in cholesteatoma: a meta-analysis. Audiol Neurootol **18:**135–142. http://dx.doi.org/10.1159/000346140.
70. **Deal C.** 2009. Future therapeutic targets in osteoporosis. Curr Opin Rheumatol **21:**380–385. http://dx.doi.org/10.1097/BOR.0b013e32832cbc2a.
71. **Asagiri M, Hirai T, Kunigami T, Kamano S, Gober H-J, Okamoto K, Nishikawa K, Latz E, Golenbock DT, Aoki K, Ohya K, Imai Y, Morishita Y, Miyazono K, Kato S, Saftig P, Takayanagi H.** 2008. Cathepsin K-dependent toll-like receptor 9 signaling revealed in experimental arthritis. Science **319:**624–627. http://dx.doi.org/10.1126/science.1150110.